VIP Membrane Fabrication

DOI: 10.1002/ange.201206640

Continuous Polycrystalline Zeolitic Imidazolate Framework-90 Membranes on Polymeric Hollow Fibers**

*Andrew J. Brown, J. R. Johnson, Megan E. Lydon, William J. Koros, Christopher W. Jones, and Sankar Nair**

The fabrication of advanced molecular separation membranes is attracting great interest because of their potential to significantly increase the energy efficiency, and reduce the cost, of renewable/clean fuel production, bio-based chemical production, greenhouse gas capture, and water purification. Currently available polymeric membranes have the advantage of low cost and high processibility. They can be engineered into different morphologies, such as asymmetric hollow fiber membranes (ca. 100–300 μm in diameter) comprised of mechanically strong macroporous fibers with a thin, dense polymeric layer that performs molecular separation.[1] These fibers are used to fabricate modules with large membrane areas in excess of $1000\ m^2 m^{-3}$ of module volume.[1,2] However, polymeric membranes are limited by an intrinsic trade-off between permeability and selectivity,[3] and higher-performance materials are desired to decisively improve the economics of emerging separation technologies. Inorganic (zeolitic) molecular sieving membranes with very high throughput and high selectivity can be fabricated by hydrothermal processing on flat and tubular ceramic supports, but currently have limited applications. This is due to the high cost of the support materials and difficulties in the scale-up and reliability of hydrothermal growth and high-temperature calcination to remove the organic structure-directing agents.[4]

Metal–organic frameworks (MOFs) are a large emerging class of crystalline nanoporous materials composed of metal centers linked by organic ligands. The synthesis and applications of MOF membranes have generated a great deal of interest.[5–21] MOFs possess attractive properties, such as fine-tuning of the pore structure by the judicious choice of metallic and organic components, and elimination of the high-temperature calcination step that is usually necessary for inorganic molecular sieving membranes. Zeolitic imidazolate frameworks (ZIFs), a subclass of MOFs, have emerged as candidates for use in the synthesis of membranes for gas and hydrocarbon separation, owing to their attractive crystallographic pore sizes (0.3–0.5 nm), and good thermal and chemical stability.[22] Taking a processing route similar to that of zeolitic membranes, several reports have described the growth and characterization of continuous polycrystalline membranes of materials such as ZIF-7, ZIF-8, ZIF-69, and ZIF-90 on ceramic (α-Al_2O_3, TiO_2) disks and tubular supports.[8–19] Further attention has been paid to the modification of ceramic support surfaces with polymeric coatings or organosilane reagents, to enhance the adhesion and growth of MOF and ZIF membranes.[7,8,11,13–19] Table S1 (see the Supporting Information) reviews currently available data[8–20] on the gas permeation characteristics of ZIF membranes in a temperature range of 25–225 °C and a pressure range of 1–3 bar. Whereas high selectivities for light gas separation have not yet been obtained, the membranes reported in the literature appear to be largely free of mesoscopic and macroscopic defects, such as pinholes and cracks. There is increasing evidence that the low gas separation selectivities in ZIF membranes investigated so far are not due to defects, but rather are related to the intrinsic properties (including flexibility and dynamics) of the ZIF crystals constituting the membrane,[23] thereby indicating that ZIFs with smaller pore sizes and less flexible structures may be more selective in gas separations. The liquid separation properties of MOFs are also attracting increased attention, and are of high interest in a number of emerging applications (for example, the separation of higher hydrocarbons or organics/water separations). Recently, it was reported that polymer/MOF mixed matrix membranes containing ZIF-8 exhibited high selectivity for alcohols over water.[24]

The scalable fabrication of MOF membranes remains a key issue, and a departure from the paradigm of ceramic-supported or dense composite membranes is needed. Herein, using ZIF-90 as an example, we show that it is possible to synthesize continuous ZIF membranes on polymeric hollow fiber surfaces by facile, low-temperature, technologically scalable methods. First, we describe the synthesis of highly uniform ZIF-90 nanocrystals (ca. 400 nm) for use as seed particles for membrane growth. A dip-coating technique is used to disperse these nanoparticles on the surfaces of macroporous hollow fibers of the poly(amide–imide) Torlon, which were fabricated by a specifically-developed fiber spinning process. Torlon was chosen as a suitable substrate polymer for separation applications because it is chemically resistant, withstands high pressures (up to 2000 psia) without plasticization, and is amenable to the engineering of hollow fibers of controlled macroporosity.[25] Thereafter, we demonstrate the growth of continuous ZIF-90

[*] A. J. Brown, M. E. Lydon
School of Chemistry and Biochemistry
Georgia Institute of Technology
901 Atlantic Drive NW, Atlanta GA 30332 (USA)
Dr. J. R. Johnson, Prof. W. J. Koros, Prof. C. W. Jones, Prof. S. Nair
School of Chemical & Biomolecular Engineering
Georgia Institute of Technology
311 Ferst Drive NW, Atlanta GA 30332 (USA)
E-mail: sankar.nair@chbe.gatech.edu

[**] This work was supported by the Phillips 66 Company.
Supporting information for this article is available on the WWW under http://dx.doi.org/10.1002/anie.201206640.

membranes on the Torlon hollow fibers by low-temperature (65 °C) liquid-phase processes, and characterize the structure and composition of the fiber-supported ZIF membranes. Finally, we report gas and liquid permeation properties of the ZIF-90/Torlon fiber membranes and briefly discuss the molecular transport mechanisms indicated by the data.

Uniform, submicron ZIF-90 seed crystals were synthesized by the addition of methanol to the synthesis as a nonsolvent (see the Experimental Section). By separating the metal source in the nonsolvent and the imidazole carboxyaldehyde ligand in dimethylformamide (DMF) until the time of mixing, small ZIF-90 crystals can be synthesized with a very narrow size distribution. Colloidal ZIF-90 seed crystals (Figure 1) with a narrow size distribution (mean = 397 nm and standard deviation = 14 nm) were produced.

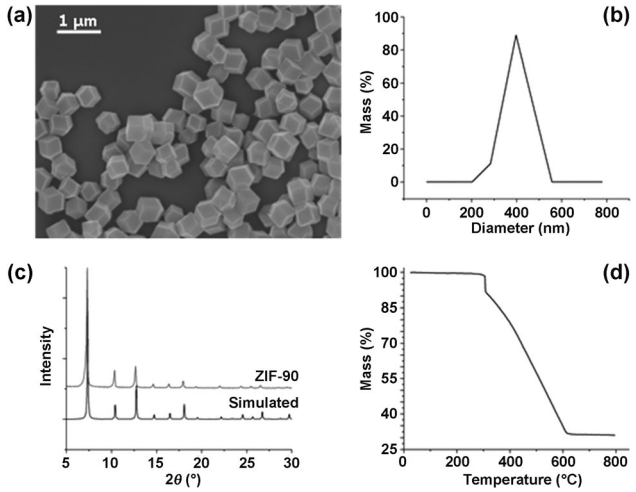

Figure 1. a) SEM Image of ZIF-90 nanocrystals, b) particle size distribution estimated from dynamic light scattering (DLS) analysis, c) XRD patterns of ZIF-90 particles and comparison to the simulated pattern of the ZIF-90 structure, and d) thermogravimetric profile of ZIF-90 particles.

XRD confirmed the presence of a highly crystalline ZIF-90 structure without any impurity phases. Based on the thermogravimetric trace, the structure is stable up to 300 °C, whereupon it decomposes. Furthermore, the solvent was easily evacuated from the pores by drying in an oven at 60 °C for 48 h. To synthesize ZIF-90/Torlon hollow fiber membranes, the ends of Torlon fiber sections (20.3 cm in length) were first sealed with epoxy to prevent crystal growth on the inner fiber surface. The Torlon hollow fibers were fabricated in-house,[26] and their porosity and surface roughness were characterized (see the Supporting Information). Attempts to grow ZIF-90 films without the presence of seed crystals on the fiber surfaces resulted in poorly intergrown crystals populating the fiber surface (see the Supporting Information). This result highlights the critical importance of seeding the fiber surface. Details of the seeding and membrane growth techniques are given in the Experimental Section. A dense layer of ZIF-90 seed crystals was deposited on the fiber surface (Figure 2 a). Highly intergrown polycrystalline membranes were obtained that covered the entire fiber surface

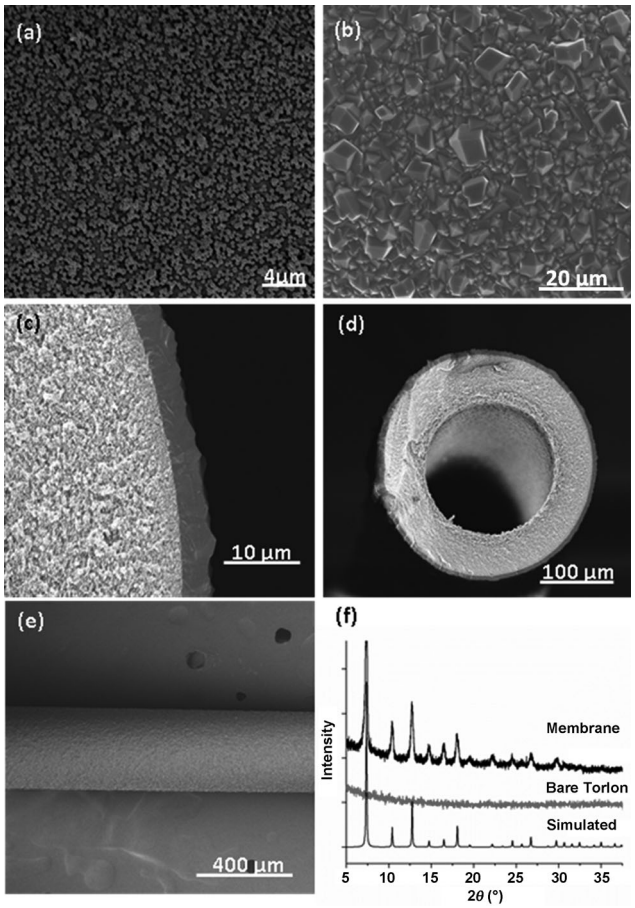

Figure 2. SEM images of: a) the ZIF-90 seed-layer, b) top view and c,d) cross section views of the polycrystalline ZIF-90 membrane after secondary growth, e) low-magnification view showing complete coverage of the fiber surface by the ZIF-90 membrane, and f) XRD patterns of bare Torlon and the membrane.

with no visible gaps, pinholes, or cracks (Figure 2 b–e). XRD confirmed the ZIF-90 crystal structure and that the membrane crystallites are randomly oriented (Figure 2 f). Membrane thicknesses were about 5 μm.

Single-gas permeation data for H_2, CO_2, N_2, CH_4, and SF_6 were collected at 35 °C using a time-lag method described elsewhere.[12,20] Single-component data for ZIF-90/Torlon membranes are displayed in Figure 3 a–c. Gases ranging in kinetic diameter from 0.28 nm (H_2) to 0.55 nm (SF_6) were used to characterize the transport mechanisms. The gases show a strong trend of decreasing permeance with increasing kinetic diameter (Figure 3 a), showing that the permeation properties are influenced by transport through the ZIF-90 pores and not through defects such as pinholes, cracks, or grain boundaries. The CO_2/N_2 and CO_2/CH_4 selectivities of 3.5 and 1.5, respectively, are comparable to previous reports on ZIF membranes (Table S1) and are well above the Knudsen selectivities (0.8 and 0.6), further confirming that gas transport is mainly through the ZIF-90 crystals. Interestingly, the CO_2/CH_4 selectivity is lower than the CO_2/N_2 selectivity. ZIF-90 and other ZIF materials are known to have high CO_2 adsorption capacities, and typically also adsorb

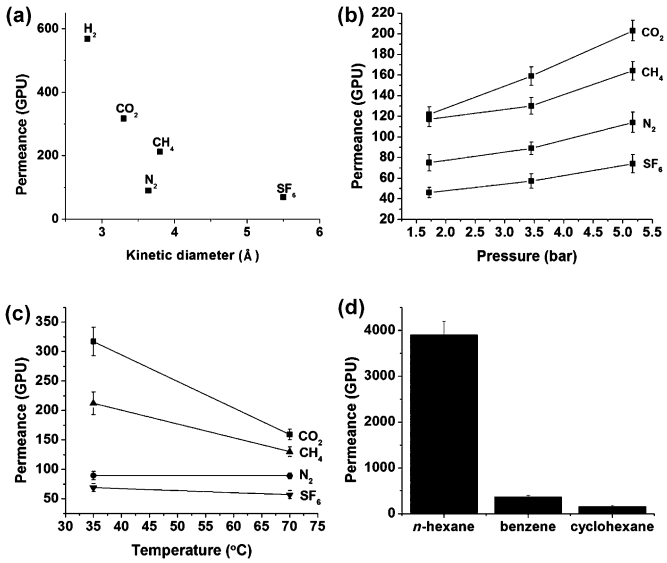

Figure 3. Permeances of gases at a) 35 °C and 50 psia as a function of kinetic diameter, b) 70 °C as a function of pressure, c) 50 psia as a function of temperature, and d) permeances of hydrocarbons at 22 °C by pervaporation. Error estimates were obtained as standard deviations from independent permeation measurements on 3 or more samples, and varied from 6% for N_2 to 11% for cyclohexane.

CH_4 more strongly than N_2.[9,23,27] Thus, the selective adsorption of gases may also contribute to the selectivity in ZIF-90 membranes, and it is not purely due to molecular sieving. This is further corroborated by the significant permeance of SF_6, the kinetic diameter of which (0.55 nm) is considerably larger than the nominal pore size of ZIF-90 (0.35 nm). The N_2/SF_6 selectivity of 1.6 is lower than the Knudsen value of 2.3. This is not due to membrane defects, since the other gas selectivities are higher than the Knudsen baseline.

To investigate further, permeation data were also collected at a higher temperature (70 °C) and at feed pressures of 25–75 psia, with the permeate being under vacuum. In Figure 3b, all of the gas permeances increase with the feed pressure at fixed temperature (70 °C); the corresponding selectivities for all gas pairs initially increase with feed pressure and then approach saturation. The permeance decreases significantly for all gases as the temperature is increased from 35 °C to 70 °C at fixed pressure (50 psia), with CO_2 showing the largest reduction (Figure 3c). The above observations are consistent with the strong role of adsorption in determining the permeation behavior, and may also indicate the influence of ZIF-90 flexibility allowing the adsorption of molecules such as SF_6 that are considerably larger than the crystallographic pore size of ZIF-90. The gas permeabilities (obtained from the permeances by multiplication by the membrane thickness) are high, and within the range shown in Table S1. For example, with a membrane thickness of 5 μm, the CO_2 permeability is 1590 Barrers at 35 °C and 50 psia feed pressure.

Recent sorption and permeation studies on ZIF-8 have shown that the effective pore size is close to 0.4 nm, making it a suitable material for the sieving of larger molecules (such as ethane/propane, propylene/propane).[28] To investigate the permeation behavior of larger molecules through ZIF-90, we also gathered data on the pervaporation of organic molecules through the ZIF-90/Torlon hollow fiber membranes (Figure 3d). Single-component pervaporation data for cyclohexane, benzene, and *n*-hexane were collected with a set-up described elsewhere.[29] The hexane permeance of a bare Torlon fiber (300000 GPU) decreased to 3900 GPU after the growth of the ZIF-90 membrane. The ZIF-90/Torlon membranes are selective for the linear *n*-hexane over cyclic hydrocarbons such as benzene and cyclohexane. Specifically, the *n*-hexane flux through the film was found to be much larger than benzene and cyclohexane, with permeances of 370 GPU and 160 GPU, respectively. This behavior is consistent with chromatography data for ZIF-8 crystals, which were used as the stationary phase in a capillary to separate linear alkanes from branched and cyclic hydrocarbons.[30]

In summary, this work demonstrates that MOF membranes can be fabricated by a technologically scalable low-temperature process on polymeric hollow fiber supports, with complete surface coverage and a lack of mesoscopic or macroscopic defects. This work leads the way to hollow-fiber MOF membranes that can be scaled up for the fabrication of high-surface-area membrane modules. The gas separation factors of the ZIF-90/Torlon membranes are modest and consistent with previous literature on ceramic-supported ZIF membranes, whereas the pervaporation properties indicate that higher permeances and selectivities are possible for ZIF-based liquid separations. The dependence of permeation rates on kinetic diameter, molecular weight, temperature, and pressure, all imply the role of adsorption phenomena in the permeation mechanism.

Experimental Section

To synthesize highly uniform ZIF-90 seeds, imidazole carboxyaldehyde (ImCA; 1.920 g, 20 mmol; Acros) was added to dimethylformamide (DMF; 50 mL) and heated to 70 °C until dissolved. After cooling to room temperature, a mixture consisting of zinc nitrate hexahydrate (1.485 g, 5 mmol; Aldrich) dissolved in methanol (50 mL) was rapidly poured into the ImCA/DMF solution and mixed for 30 min. ZIF-90 crystals were separated from the cloudy suspension by three cycles of centrifugation and washing in methanol. XRD patterns were collected with a Phillips X'Pert diffractometer equipped with an RTMS (X'Celerator) detector using $Cu_{K\alpha}$ radiation. A LEO-1550 SEM was used to collect images of powders and films after a thin layer of gold was sputtered onto the sample surface. Dynamic light scattering (DLS) measurements were conducted with a Protein Solutions DynaPro DLS instrument. Particles were dispersed in methanol and then transferred to a cuvette with a 5 micron syringe filter. A Netzsch STA 409 PG Luxx was used for thermogravimetric analysis (TGA). The fibers were seeded by dip-coating into a ZIF-90/ethanol suspension (4 $g L^{-1}$) and air-dried for 30 min before secondary growth. For fabricating ZIF-90 membranes, the growth solution was prepared by first adding ImCA (960 mg) to methanol (100 mL), followed by sonication until the ligand dissolved. Then, the solution was cooled to room temperature and zinc nitrate hexahydrate (740 mg) was added. The growth solution was then poured into a 100 mL KIMAX test tube to which a seeded fiber was then added. The tube was then capped and heated in a convection

oven to 65 °C. After 4 h, the tube was cooled under ambient conditions, and the fiber was thoroughly rinsed with methanol.

Received: August 17, 2012
Published online: September 26, 2012

Keywords: gas separation · hollow fibers · membranes · metal–organic framework · pervaporation

[1] R. Baker, *Membrane Technology and Applications*, *2nd ed.*, Wiley, Hoboken, **2004**.
[2] W. J. Koros, R. Mahajan, *J. Membr. Sci.* **2000**, *175*, 181 – 196.
[3] a) B. D. Freeman, *Macromolecules* **1999**, *32*, 375 – 380; b) L. M. Robeson, *J. Membr. Sci.* **1991**, *62*, 165 – 185.
[4] a) M. A. Carreon, S. G. Li, J. L. Falconer, R. D. Noble, *J. Am. Chem. Soc.* **2008**, *130*, 5412 – 5413; b) T. Tomita, K. Nakayama, H. Sakai, *Microporous Mesoporous Mater.* **2004**, *68*, 71 – 75.
[5] a) J. Gascon, S. Aguado, F. Kapteijn, *Microporous Mesoporous Mater.* **2008**, *113*, 132 – 138; b) V. V. Guerrero, Y. Yoo, M. C. McCarthy, H. K. Jeong, *J. Mater. Chem.* **2010**, *20*, 3938 – 3943.
[6] Y. Yoo, Z. P. Lai, H. K. Jeong, *Microporous Mesoporous Mater.* **2009**, *123*, 100 – 106.
[7] R. Ranjan, M. Tsapatsis, *Chem. Mater.* **2009**, *21*, 4920 – 4924.
[8] Y. S. Li, F. Y. Liang, H. Bux, A. Feldhoff, W. S. Yang, J. Caro, *Angew. Chem.* **2010**, *122*, 558 – 561; *Angew. Chem. Int. Ed.* **2010**, *49*, 548 – 551.
[9] a) Y. Y. Liu, E. P. Hu, E. A. Khan, Z. P. Lai, *J. Membr. Sci.* **2010**, *353*, 36 – 40; b) Y. Y. Liu, G. F. Zhang, Y. C. Pan, Z. P. Lai, *J. Membr. Sci.* **2011**, *379*, 46 – 51.
[10] S. R. Venna, M. A. Carreon, *J. Am. Chem. Soc.* **2010**, *132*, 76 – 78.
[11] H. Bux, F. Y. Liang, Y. S. Li, J. Cravillon, M. Wiebcke, J. Caro, *J. Am. Chem. Soc.* **2009**, *131*, 16000 – 16001.
[12] M. C. McCarthy, V. Varela-Guerrero, G. V. Barnett, H.-K. Jeong, *Langmuir* **2010**, *26*, 14636 – 14641.
[13] H. Bux, A. Feldhoff, J. Cravillon, M. Wiebcke, Y.-S. Li, J. Caro, *Chem. Mater.* **2011**, *23*, 2262 – 2269.
[14] A. Huang, W. Dou, J. Caro, *J. Am. Chem. Soc.* **2010**, *132*, 15562 – 15564.
[15] A. Huang, J. Caro, *Angew. Chem.* **2011**, *123*, 5083 – 5086; *Angew. Chem. Int. Ed.* **2011**, *50*, 4979 – 4982.
[16] A. Huang, H. Bux, F. Steinbach, J. Caro, *Angew. Chem.* **2010**, *122*, 5078 – 5081.
[17] G. Xu, J. Yao, K. Wang, L. He, P. A. Webley, C. S. Chen, H. Wang, *J. Membr. Sci.* **2011**, *385 – 386*, 187 – 193.
[18] Y. S. Li, F. Y. Liang, H. Bux, W. S. Yang, J. Caro, *J. Membr. Sci.* **2010**, *354*, 48 – 54.
[19] S. Aguado, C. H. Nicolas, V. Moizan-Basle, C. Nieto, H. Amrouche, N. Bats, N. Audebrand, D. Farrusseng, *New J. Chem.* **2011**, *35*, 41 – 44.
[20] S. W. Rutherford, D. D. Do, *Adsorption* **1997**, *3*, 283 – 312.
[21] M. Shah, M. C. McCarthy, S. Sachdeva, A. K. Lee, H. K. Jeong, *Ind. Eng. Chem. Res.* **2012**, *51*, 2179 – 2199.
[22] a) K. S. Park, Z. Ni, A. P. Cote, J. Y. Choi, R. D. Huang, F. J. Uribe-Romo, H. K. Chae, M. O'Keeffe, O. M. Yaghi, *Proc. Natl. Acad. Sci. USA* **2006**, *103*, 10186 – 10191; b) W. Morris, C. J. Doonan, H. Furukawa, R. Banerjee, O. M. Yaghi, *J. Am. Chem. Soc.* **2008**, *130*, 12626 – 12627.
[23] a) H. Amrouche, S. Aguado, J. Perez-Pellitero, C. Chizallet, F. Siperstein, D. Farrusseng, N. Bats, C. Nieto-Draghi, *J. Phys. Chem. C* **2011**, *115*, 16425 – 16432; b) D. Fairen-Jimenez, S. A. Moggach, M. T. Wharmby, P. A. Wright, S. Parsons, T. Duren, *J. Am. Chem. Soc.* **2011**, *133*, 8900 – 8902; c) H. L. Huang, W. J. Zhang, D. H. Liu, B. Liu, G. J. Chen, C. L. Zhong, *Chem. Eng. Sci.* **2011**, *66*, 6297 – 6305.
[24] X. L. Liu, Y. S. Li, G. Q. Zhu, Y. J. Ban, L. Y. Xu, W. S. Yang, *Angew. Chem.* **2011**, *123*, 10824 – 10827; *Angew. Chem. Int. Ed.* **2011**, *50*, 10636 – 10639.
[25] M. R. Kosuri, W. J. Koros, *J. Membr. Sci.* **2008**, *320*, 65 – 72.
[26] M. R. Kosuri, W. J. Koros, *J. Membr. Sci.* **2008**, *23*, 3025 – 3028.
[27] A. Venkatasubramanian, M. Navaei, K. R. Bagnall, K. C. McCarley, S. Nair, P. J. Hesketh, *J. Phys. Chem. C* **2012**, *116*, 15313 – 15321.
[28] a) Y. Pan, Z. Lai, *Chem. Commun.* **2011**, *47*, 10275 – 10277; b) Y. Dai, J. R. Johnson, O. Karvan, D. S. Sholl, W. J. Koros, *J. Membr. Sci.* **2012**, *401*, 76 – 82; c) Y. Pan, T. Li, G. Lestari, Z. Lai, *J. Membr. Sci.* **2012**, *390 – 391*, 93 – 98; d) C. Zhang, R. P. Lively, K. Zhang, J. R. Johnson, O. Karvan, W. J. Koros, *J. Phys. Chem. Lett.* **2012**, *3*, 2130 – 2134.
[29] W. L. Qiu, M. Kosuri, F. B. Zhou, W. J. Koros, *J. Membr. Sci.* **2009**, *327*, 96 – 103.
[30] a) N. Chang, Z.-Y. Gu, X.-P. Yan, *J. Am. Chem. Soc.* **2010**, *132*, 13645 – 13647; b) A. Demessence, C. Boissiere, D. Grosso, P. Horcajada, C. Serre, G. Ferey, G. J. A. A. Soler-Illia, C. Sanchez, *J. Mater. Chem.* **2010**, *20*, 7676 – 7681; c) M. T. Luebbers, T. Wu, L. Shen, R. I. Masel, *Langmuir* **2010**, *26*, 15625 – 15633.